CHEMISTRY OF MATERIALS

ARTICLE

pubs.acs.org/cm

New Poly(arylene vinylene)s Based on Diketopyrrolopyrrole for Ambipolar Transistors

Pei-Tzu Wu,[†] Felix Sunjoo Kim,[†] and Samson A. Jenekhe*[,†,‡]

[†]Department of Chemical Engineering and [‡]Department of Chemistry, University of Washington, Seattle, Washington 98195-1750, United States

Supporting Information

ABSTRACT: Three diketopyrrolopyrrole-based donor−acceptor copolymer semiconductors were synthesized by Stille coupling polymerization and their structural, photophysical, electrochemical, and field-effect charge transport properties were characterized. The new copolymers, poly[3,6-(2,5-bis(2-hexyldecyl)pyrrolo[3,4-*c*]pyrrole-1,4-dione)-*alt*-1,2-bis-(2′-thienyl)vinyl-5′,5″-diyl] (HD-PPTV), poly[3,6-(2,5-bis(2-hexyldecyl)-pyrrolo[3,4-*c*]pyrrole-1,4-dione)-*alt*-1,2-bisphenylvinyl-4′,4″-diyl] (HD-PPPV), and a 50:50 random copolymer (PPTPV), have moderate number-average molecular weights (21800−88800 g/mol). The copolymers have optical absorption bands in the visible to near-IR regions with optical bandgaps that varied from 1.22 eV for HD-PPTV to 2.0 eV for HD-PPPV. Ionization potentials of 5.14−5.48 eV and electron affinities of 3.13−3.34 eV were derived from cyclic voltammetry. Ambipolar charge transport was seen in transistors based on HD-PPTV and PPTPV, whereas only hole transport was observed in HD-PPPV. Field-effect transistors fabricated from HD-PPTV had hole and electron mobilities as high as 0.2 and 0.03 $cm^2\ V^{-1}\ s^{-1}$. Integration of the ambipolar HD-PPTV transistors into complementary inverters demonstrated sharp switching characteristics with large voltage gains of up to 27.

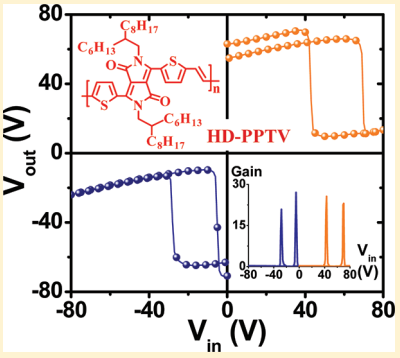

KEYWORDS: diketopyrrolopyrrole, poly(arylene vinylene), ambipolar charge transport, field-effect transistor, complementary inverter

INTRODUCTION

Conjugated copolymers with donor−acceptor (D−A) architectures are of much interest because their modular design allow for facile tailoring of their electronic structure, including the highest occupied molecular orbital (HOMO) and lowest unoccupied molecular orbital (LUMO) energy levels, the energy bandgap, and the photon absorption in a broad wavelength region.[1−3] The independent selection of the electron donor or electron acceptor moiety in the conjugated D−A copolymers can facilitate the independent tuning of the HOMO and LUMO energy levels.[1−3] For example, the incorporation of a strong electron-withdrawing acceptor moiety in a D−A copolymer can usually give rise to a low-lying LUMO (high electron affinity), a high-lying HOMO (low ionization potential), and small bandgap energy.[3] D−A conjugated copolymers containing strong electron acceptors bearing imide or lactam groups, such as naphthalene bisimide and diketopyrrolopyrrole, have recently been found to exhibit strong intramolecular charge transfer, leading to excellent intramolecular planarity, intense broad absorption from the visible to the near-infrared, large electron affinity (EA > 3.4 eV), and good electron transport.[2,4,5] Furthermore, the solubility can be enhanced or tailored by the choice of N-substituent on the imide or lactam rings.

There is a growing interest in D−A conjugated polymers[5−8] and oligomers[9] incorporating 1,4-diketo-2,5-dihydropyrrolo-[3,4-*c*]pyrrole (DPP) as an electron-accepting building block. DPP-based polymers and oligomers have been shown to exhibit efficient luminescence,[6] good field-effect charge transport,[5,8] and small bandgaps ($E_g^{opt} \sim 1.1−1.8$ eV),[7,8] which have been exploited in organic light-emitting diodes,[6] thin film transistors,[5,8] and solar cells.[7−9] A wide variety of aryl-DPP-aryl compounds have been synthesized and used as organic pigments.[10a] Chemical modifications on aryl−DPP−aryl, including varying the substituent at the 2,5-position of the DPP unit or changing the neighboring aryl groups, can lead to a change in solubility, planarity,[9] hydrogen-bonding interactions,[10] self-assembly,[9,10] conjugation length,[9,10] and electronic structure.[9,10] DPP-based polymers that contain a 1,4-diketo-3,6-bis(thien-2-yl)pyrrolo[3,4-c]pyrrole (Th−DPP−Th) core have been shown to exhibit field-effect hole mobilities of 0.1 $cm^2\ V^{-1}\ s^{-1}$.[5] Most of the reported D−A copolymers based on DPP showed good mobility of holes (>10^{-3} $cm^2\ V^{-1}\ s^{-1}$).[5,7,8] A few DPP-based conjugated copolymers show ambipolar charge transport with hole mobilities of 10^{-5} to 0.11 $cm^2\ V^{-1}\ s^{-1}$ and electron mobilities of 4.2×10^{-6} to 0.09 $cm^2\ V^{-1}\ s^{-1}$.[5,8a,8f,8g] Among the diketopyrrolopyrrole-containing copolymers that show ambipolar charge transport, only two of them had a high hole mobility of 0.11 $cm^2\ V^{-1}\ s^{-1}$,

Received: August 1, 2011
Revised: September 3, 2011
Published: September 30, 2011

whereas the electron mobility was 0.003−0.09 $cm^2 V^{-1} s^{-1}$.[5,8g] The power conversion efficiency of bulk heterojunction solar cells based on DPP-containing polymers and fullerene derivatives has reached up to 4.7%.[8a] More recently, DPP-based conjugated copolymers having unipolar hole transport with a hole mobility of 1.0−1.4 $cm^2 V^{-1} s^{-1}$ and ambipolar charge transport with hole and electron mobilities as high as 0.3−0.4 $cm^2 V^{-1} s^{-1}$ have been reported.[8h−j]

Herein, we report the synthesis and investigation of the photophysical, electrochemical, and field-effect charge transport properties of three new poly(arylene vinylene)s based on the 1,4-diketo-2,5-dihydropyrrolo[3,4-*c*]pyrrole (DPP) unit. The choice of arylene vinylene linkage was intended to impart a stronger electron-donating feature in such donor−acceptor copolymers compared to their arylene-linked analogs. The molecular structures of the new DPP-containing D−A copolymers, poly[3,6-(2,5-bis(2-hexyldecyl)pyrrolo[3,4-*c*]pyrrole-1,4-dione)-*alt*-1,2-bis-(2′-thienyl)vinyl-5′,5″-diyl] (HD-PPTV), poly[3,6-(2,5-bis(2-hexyldecyl)-pyrrolo[3,4-*c*]pyrrole-1,4-dione)-*alt*-1,2-bisphenylvinyl-4′,4″-diyl]- (HD-PPPV), and a 50:50 random copolymer (PPTPV), are shown in Chart 1. The morphology of solution-cast films of the DPP-based poly(arylene vinylene)s was investigated by X-ray diffraction. The electronic structure (HOMO/LUMO levels) of the new polymers was estimated by performing cyclic voltammetry on thin films. The expected increase in the strength of intramolecular charge transfer (ICT) in going from the phenylene vinylene-linked HD-PPPV to the thiophene vinylene-linked HD-PPTV should allow a study of the effects of ICT strength on not only electronic structure but also charge transport in diketopyrrolopyrrole-containing poly(arylene vinylene)s. Indeed, *unipolar* charge transport was observed in HD-PPPV OFETs, whereas high-mobility *ambipolar* charge transport was observed in HD-PPTV OFETs. The high-mobility (∼0.2 $cm^2 V^{-1} s^{-1}$ for holes and 0.03 $cm^2 V^{-1} s^{-1}$ for electrons) ambipolar HD-PPTV OFETs were integrated into complementary-like inverters, resulting in sharp switching characteristics and good voltage gains (∼27) in the logic circuits.

Chart 1. Molecular Structures of New Poly(arylene vinylene)s

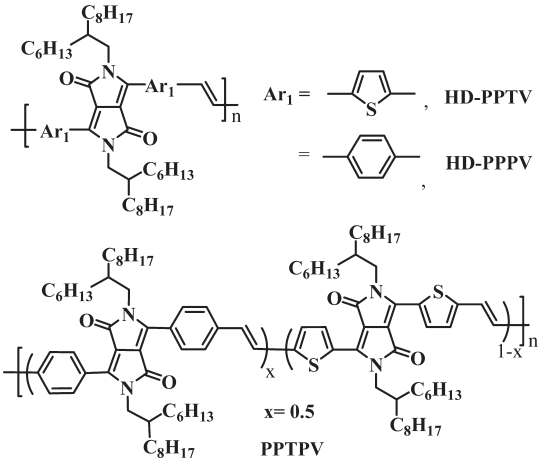

EXPERIMENTAL SECTION

Materials. *trans*-1,2-Bis(tributylstannyl)ethylene was purchased from Alfa Aesar and used as received. Anhydrous chlorobenzene and other chemicals were purchased from Aldrich and used as received. 2-Hexyldecyl bromide,[11a] 3,6-bis(5-bromo-thiophen-2-yl)-2,5-bis(2-hexyldecyl)-pyrrolo[3,4-*c*]pyrrole-1,4-dione (**1**),[5,8a] and 3,6-bis(4-bromophenyl)-2,5-bis(2-hexyldecyl)pyrrolo[3,4-*c*]pyrrole-1,4-dione (**2**)[10b] were synthesized following the literature methods. The ^{1}H NMR spectra of **1** and **2** are provided in the Supporting Information (Figure S1).

3,6-Bis(5-bromo-thiophen-2-yl)-2,5-bis(2-hexyldecyl)pyrrolo[3,4-*c*]-pyrrole-1,4-dione (**1**): ^{1}H NMR ($CDCl_3$), δ (ppm) 8.55 (m, 2H), 7.15 (m, 2H), 3.85 (d, 4H), 1.81 (s, 2H), 1.38−1.03 (m, 48H), 0.88 (t, 12H). 3,6-Bis(4-bromophenyl)-2,5-bis(2-hexyldecyl)pyrrolo[3,4-*c*]pyrrole-1,4-dione (**2**): ^{1}H NMR ($CDCl_3$), δ (ppm) 7.69 (m, 8H), 3.73 (d, 4H), 1.35−1.05 (m, 50H), 0.89 (t, 12H).

Synthesis of DPP-Based Poly(arylene vinylene)s. Three polymers were prepared by Stille coupling polymerization of monomer **1** or **2** with *trans*-1,2-bis(tributylstannyl)ethylene as shown in Scheme 1.[11b] The general polymerization procedure in the synthesis of the DPP-based poly(arylene vinylene)s is given below using the synthesis of HD-PPTV as an example.

Poly[3,6-(2,5-bis(2-hexyldecyl)pyrrolo[3,4-*c*]pyrrole-1,4-dione)-*alt*-1,2-bis-(2′-thienyl)vinyl-5′,5″-diyl] (HD-PPTV). 3,6-Bis(5-bromo-thiophen-2-yl)-2,5-bis(2-hexyldecyl)pyrrolo[3,4-*c*]

Scheme 1. Synthesis of DPP-Based Poly(arylene vinylene)s

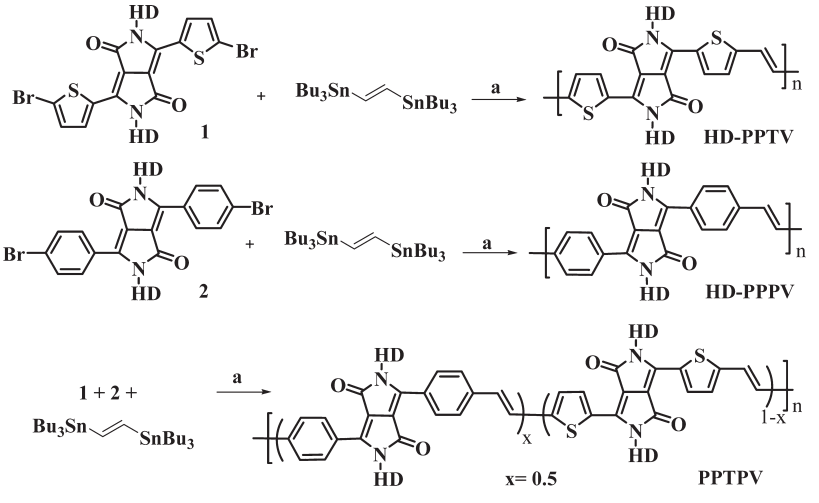

dx.doi.org/10.1021/cm202247a |*Chem. Mater.* 2011, 23, 4618–4624

Table 1. Molecular Weights and Electronic Structure of DPP-Based Poly(arylene vinylene)s

polymer	M_w (g/mol)	M_n (g/mol)	PDI	E_g^{opt} (eV)	E_{onset}^{red} [a] (V)	EA [b] (eV)	E_{onset}^{ox} [a] (V)	IP [c] (eV)	E_g^{el} (eV)
HD-PPPV	206 000	88 800	2.32	2.00	−1.27	3.13	1.08	5.48	2.35
HD-PPTV	154 000	56 200	2.74	1.22	−1.06	3.34	0.74	5.14	1.80
PPTPV	78 500	21 800	3.60	1.26	−1.09	3.31	0.81	5.21	1.90

[a] Onset oxidation and reduction potentials vs SCE. [b] Electron affinity was obtained based on EA = eE_{red}^{onset} + 4.4 eV. [c] Ionization potential was obtained based on IP = eE_{ox}^{onset} + 4.4 eV.

pyrrole-1,4-dione (**1**) (480 mg, 0.53 mmol) and *trans*-1,2-bis(tributylstannyl)ethylene (320.8 mg, 0.53 mmol) were dissolved in anhydrous chlorobenzene (18 mL) and purged with Ar. The catalyst, $Pd_2(dba)_3$ (9.7 mg, 0.01 mmol), and the ligand P(*o*-toyl)$_3$ (12.9 mg, 0.04 mmol) were added and degassed. After being purged with Ar for 5 min, the solution was refluxed at 120 °C for 2 days (48 h). The solution was then quenched by cooling and then precipitated into methanol. The solid was filtered and underwent Soxhlet extraction with acetone and dried in a vacuum oven to afford a dark green solid (398 mg, yield: 95%). ^{1}H NMR ($CDCl_3$), δ (ppm): 8.93 (br, 2H), 7.01 (br, 4H), 4.09 (br, 4H), 1.97 (br, 2H), 1.25 (48H), 0.87 (br, 12H).

Poly[3,6-(2,5-bis(2-hexyldecyl)pyrrolo[3,4-c]pyrrole-1,4-dione)-*alt*-1,2-bisphenylvinyl-4′,4″-diyl] (HD-PPPV). Purple solid, yield: 47%. ^{1}H NMR ($CDCl_3$), δ (ppm): 7.63 (br, 8H), 7.09 (br, 2H), 3.85 (br, 4H), 1.7−1.25 (br, 50H), 0.89 (br, 12H).

Poly{[3,6-(2,5-bis(2-hexyldecyl)pyrrolo[3,4-*c*]pyrrole-1,4-dione)-*alt*-1,2-bisphenylvinyl-4′,4″-diyl]-*co*-3,6-(2,5-bis(2-hexyldecyl)pyrrolo[3,4-*c*]pyrrole-1,4-dione)-*alt*-1,2-bis-(2′-thienyl)vinyl-5′,5″-diyl]} (PPTPV). Black solid, yield: 33%. ^{1}H NMR ($CDCl_3$), δ (ppm): 8.92 (br, 1H), 7.84−6.74 (br, 7H), 4.07 (br, 2H), 3.82 (br, 2H), 1.94−1.25 (br, 49H), 0.87 (br, 12H). The actual composition (x) of the random copolymer was calculated to be 0.5 using integration of the α-methylene proton resonance as follows: $x = \delta$ (4.07)/[δ (4.07) + δ (3.82)].

Sample Preparation for X-ray Diffraction. Each copolymer was dissolved in a chloroform/chlorobenzene mixture (1:2, vol:vol) at 10−20 mg/mL and the solutions were drop cast onto glass substrates. The films were then dried on a hot plate at 60 °C in air.

Characterization. ^{1}H NMR spectra were recorded on a Bruker-AF300 spectrometer at 300 MHz. UV−visible absorption spectra were recorded on a Perkin-Elmer model Lambda 900 UV/vis/near-IR spectrophotometer. The photoluminescence (PL) emission spectra were obtained with a Photon Technology International (PTI) Inc. model QM-2001-4 spectrofluorometer. The molecular weights reported for the polymers were determined on a Polymer Lab gel permeation chromatograph (GPC) Model 120 (DRI, PL-BV400HT Viscometer) against polystyrene standards in chlorobenzene at 60 °C. X-ray diffraction (XRD) patterns were obtained on a Bruker AXS D8 Focus diffractometer with Cu Kα beam (40 kV, 40 mA; λ = 0.15418 nm). Data were obtained from 2θ angles of 2−35° at a scan rate of 0.01°/s. The d-spacing was calculated from the equation $n\lambda = 2d \sin\theta$. Differential scanning calorimetry (DSC) scans were obtained on TA Instrument model Q20 DSC at a heating rate of 10 °C/min. Cyclic voltammetry experiments were done on an EG&G Princeton Applied Research Potentiostat/Galvanostat (Model 273A) using 0.1 M tetrabutylammonium hexafluorophosphate (Bu_4NPF_6) in acetonitrile as the electrolyte. A three-electrode cell was used in all experiments. Platinum wire electrodes were used as both counter and working electrodes and silver/silver ion (Ag in 0.1 M $AgNO_3$ solution, Bioanalytical System, Inc.) was used as a reference electrode. The Ag/Ag^+ ($AgNO_3$) reference electrode was calibrated at the beginning of the experiments by running cyclic voltammetry on ferrocene as the internal standard. The potential values obtained in reference to Ag/Ag^+ electrode were then converted to the saturated calomel electrode (SCE) scale. The films of the polymers were coated onto the working electrode by dipping a Pt wire into a 10 wt % solution in chloroform/chlorobenzene (1:2, vol:vol) and drying for 30 min.

Fabrication and Characterization of Field-Effect Transistors and Inverters. Field-effect transistors were fabricated on heavily doped silicon substrates with thermally grown silicon dioxide gate insulator (200 nm). Gold electrodes (40 nm) with chromium adhesive layer (2 nm) acted as the source and drain electrodes in the bottom-contact/bottom-gate transistors, forming the channel widths (W) of 400−800 μm and lengths (L) of 20−40 μm (W/L = 20). The substrates were cleaned by ultrasonication with acetone and isopropyl alcohol and dried by flow of nitrogen. The surface of a silicon dioxide substrate was treated with octyltrichlorosilane (OTS-8) to form a hydrophobic self-assembled monolayer (SAM). Each DPP polymer was deposited on the substrates by spin-coating from a solution in 1,2-dichlorobenzene (ODCB). The devices were annealed at various temperatures under inert (nitrogen) conditions. Complementary inverters were fabricated on a substrate with larger channel dimensions (W = 5000 μm and L = 100 μm). Electrical characteristics of the devices were measured by using a HP4145B semiconductor parameter analyzer under a nitrogen atmosphere. The field-effect mobility was calculated by using the saturation-region equation.

RESULTS AND DISCUSSION

Synthesis of DPP-Based Poly(arylene vinylene)s. The new poly(arylene vinylene)s based on diketopyrrolopyrrole (DPP) were prepared by Stille coupling polymerization of *trans*-1,2-bis(tributylstannyl)ethylene with the dibromides **1** or **2** as shown in Scheme 1. In the case of the random copolymer PPTPV, the two dibromides **1** and **2** at a molar feed ratio of 1:1 were used. The actual composition (x) of the random copolymer was determined to be 0.5 by using the two different resonances of α-methylene protons of *N*-(2-hexyldecyl) (δ = 4.07 and 3.82 ppm) that are characteristic of thiophene−diketopyrrolopyrrole−thiophene (Th−DPP−Th) and phenyl−diketopyrrolopyrrole−phenyl (Ph−DPP−Ph) units, respectively. Both HD-PPTV and PPTPV have good solubility in common organic solvents (chloroform, chlorobenzene, and 1,2-dichlorobenzene) at high concentrations (10−20 mg/mL), whereas HD-PPPV shows poor solubility (<2 mg/mL) in the same solvents. The number-average molecular weights (M_n) of the three vinylene copolymers are in the range of 21 800−88 800 g/mol with polydispersity indices (PDI) of 2.32−3.60 as summarized in Table 1. Interestingly, no clear thermal transition was observed for the three poly(arylene vinylene)s by differential scanning calorimetry scans in the 0 to 350 °C range (Figure S2). However, the lack of any clear glass or melting transition in the DSC scans of HD-PPTV, HD-PPPV, and PPTPV imply that thermal annealing may not substantially affect the morphology or structural order, and thus charge transport of these polymer semiconductors.

Photophysical Properties. The absorption spectra of the three DPP polymers in dilute toluene solution (1×10^{-6} to 1×10^{-5} M) and as thin films are shown in Figure 1. In solution,

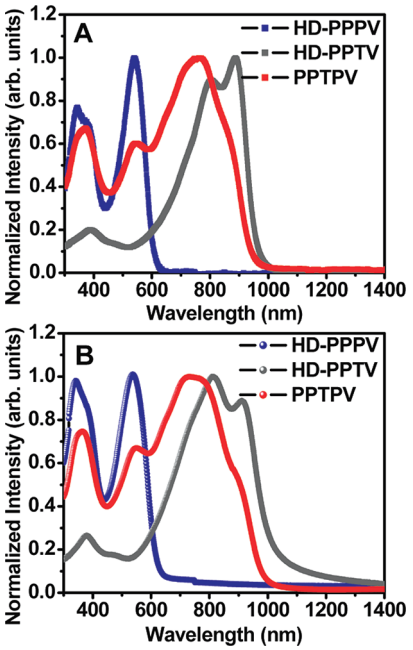

Figure 1. Optical absorption spectra of DPP polymers in dilute toluene solutions (A) and as thin films (B).

HD-PPPV and HD-PPTV have absorption maximum (λ_{max}) at 538 and 887 nm, respectively. As thin films, HD-PPPV and HD-PPTV have absorption λ_{max} at 537 and 814 nm, respectively. HD-PPPV has an optical bandgap (E_g^{opt}) of 2.0 eV, which is smaller than the reported 2.1 eV for poly(1,4-diketo-2,5-dialkyl-3,6-diphenylpyrrolo[3,4-*c*]pyrrole) because of the insertion of vinylene linkage in the repeat unit.[12a] Similarly, HD-PPTV has an optical bandgap of 1.22 eV, which is almost the same as the reported 1.25 eV for poly(1,4-diketo-2,5-dioctyl-3,6-bis(thiophen-5-yl)-pyrrolo[3,4-*c*]pyrrole).[8a] Clearly, HD-PPTV shows a much red-shifted absorption with a smaller optical bandgap (1.22 eV) compared to HD-PPPV (2.0 eV) because of the stronger intramolecular charge transfer between the thiophene (Th) donor and the diketopyrrolopyrrole (DPP) moiety compared to the phenyl (Ph) groups in HD-PPPV. We note that the absorption spectra of HD-PPTV in the solution and as thin film are both structured, which is likely caused by the exciton delocalization in an ordered chromophore system.[13]

The random copolymer PPTPV contains both chromophores of HD-PPPV and HD-PPTV. In solution, PPTPV has a broad absorption with a λ_{max} at 762 nm, characteristic of HD-PPTV, and two lower wavelength bands at 371 and 545 nm, which are reminiscent of HD-PPPV. The thin film absorption spectrum of PPTPV is similarly broad with a λ_{max} at 729 nm and two lower wavelength bands at 364 and 550 nm. A shoulder peak at 890 nm was also observed in the solution and thin film absorption spectra of PPTPV. A similar and small optical bandgap of 1.26 eV was observed and this is very close to that seen in HD-PPTV. The random copolymer has thus enabled the achievement of broad and complementary absorption in the visible and near-IR wavelengths regions beyond what is observed in HD-PPTV and HD-PPPV.

The photoluminescence (PL) emission spectra of HD-PPPV and PPTPV are shown in Figure 2. However, the PL emission spectrum of HD-PPTV could not be obtained since it falls in the near IR region, which is beyond the detection limit of our instrument.

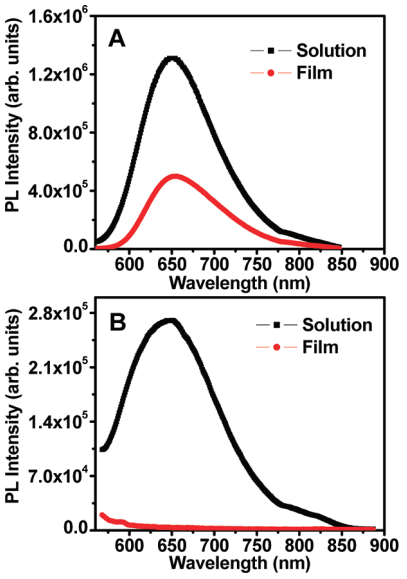

Figure 2. Photoluminescence spectra of (A) HD-PPPV and (B) PPTPV in dilute toluene solutions and as thin films.

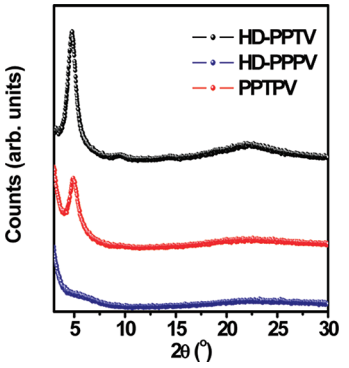

Figure 3. X-ray diffraction patterns of drop-cast films of DPP-based polymers.

HD-PPPV is weakly red-emitting with a PL emission maximum at 647 and 653 nm in dilute solution and as thin film, respectively. This HD-PPPV polymer has a large Stokes shift of 109 and 116 nm in dilute solution and as thin films similar to other DPP-based polymers.[12] Similar to HD-PPPV, the random copolymer PPTPV has a weak PL emission with a peak centered at 651 nm in dilute solution but the photoluminescence is completely quenched in the thin film. It is known that in general the PL emission of polymers with donor−acceptor architecture is less efficient when the intramolecular charge transfer is very strong.[1] Furthermore, the PL emission of conjugated polymers in the solid state can be further reduced or quenched because of strong intermolecular interactions and associated lower energy states (excimers, etc).[14]

Crystallinity of DPP-Based Poly(arylene vinylene)s. The crystalline nature of the three poly(arylene vinylene)s was investigated by X-ray diffraction (XRD) and the XRD patterns are shown in Figure 3. HD-PPTV has a (100) reflection peak at 4.78°, corresponding to a d_{100} spacing of 18.47 Å. This d_{100} spacing corresponds to a stacking distance in the lamellar packing structure, dictated by the bulky 2-hexyldecyl (HD) side chains. The broad band centered at 22.67° is related to the $\pi-\pi$ stacking

dx.doi.org/10.1021/cm202247a |*Chem. Mater.* 2011, 23, 4618–4624

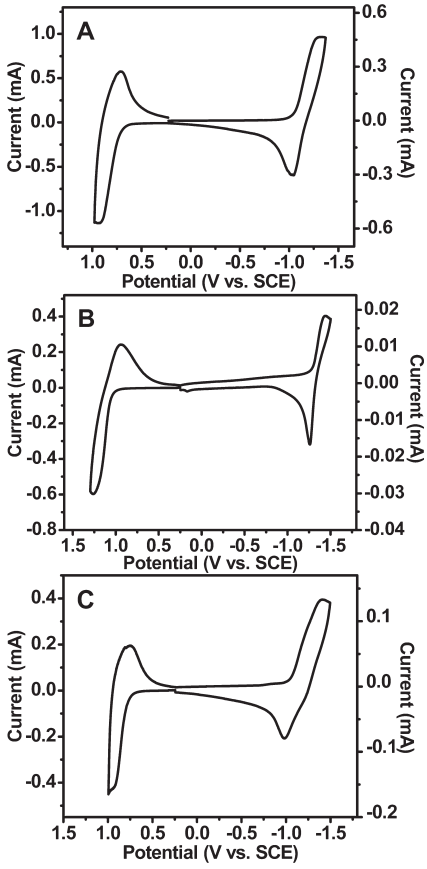

Figure 4. Cyclic voltammograms of HD-PPTV (A), HD-PPPV (B), and PPTPV (C).

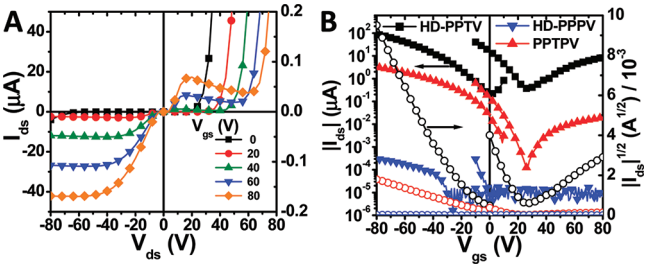

Figure 5. (A) Output characteristics of the field-effect transistor based on HD-PPTV after annealing at 150 °C. (B) Overlays of transfer curves (V_{ds}= ± 80 V) of the transistors of HD-PPTV, HD-PPPV, and PPTPV.

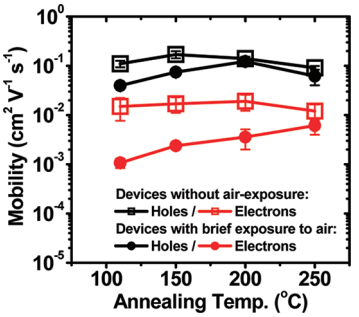

Figure 6. Effects of the annealing temperature and air exposure on hole and electron mobilities of HD-PPTV.

distance (3.92 Å). This result reveals that the HD-PPTV copolymer films exhibit a lamellar crystalline packing. However, HD-PPPV did not show any reflection peak in the XRD pattern, which suggests an amorphous film. Interestingly, the random copolymer PPTPV shows a weak reflection peak at 4.89°, corresponding to a d_{100} spacing of 18.02 Å. This means that PPTPV has a lamellar packing structure similar to HD-PPTV and thus a degree of crystallinity. Observation of crystallinity in random copolymer PPTPV with a statistical distribution of the π-conjugated main chain segments is to be contrasted with recently discovered high crystallinity in random copoly(3-alkylthiophene)s with multiple different-sized side chains.[15] Previously, various DPP-based copolymers bearing the same Th−DPP−Th core with HD-PPTV were also reported to form a lamellar crystalline packing structure with an interlayer stacking distance (d_{100}) of 14.8−18.2 Å, depending on the substituted side chains along the conjugated main chains.[8d,g]

The Th−DPP−Th core of HD-PPTV is known to be highly planar, which facilitates charge delocalization, strong $\pi-\pi$ stacking, and efficient charge transport.[9] Theoretically, a short distance (2.1 Å) is estimated between the carbonyl oxygen of DPP and adjacent thiophene hydrogen, which is considered favorable for intramolecular and intermolecular hydrogen-bonding interactions in the Th−DPP−Th core.[16] On the other hand, a large torsion angle between the phenyl groups and the DPP unit in the Ph−N-alkylated DPP−Ph units was predicted by density functional theory.[17] Also, the phenyl group rotation leads to the loss of planarity and significantly decreases the overlap between π-orbitals of phenyl and DPP groups.[17] The nonplanar structure of the Ph−DPP−Ph core in HD-PPPV results in less efficient $\pi-\pi$ stacking and lower structural order and this may explain the absence of reflection peaks in its X-ray diffraction pattern.

Electrochemical Properties. Cyclic voltammetry (CV) was performed to evaluate the electronic structure (EA and IP). Both reduction and oxidation waves in the CV scans of the three copolymers showed quasi-reversible processes as shown in Figure 4. The ionization potential (IP) and electron affinity (EA) estimated from the CVs[18,19] are summarized in Table 1. HD-PPPV has a large ionization potential of 5.48 eV compared to HD-PPTV (5.14 eV) and PPTPV (5.21 eV). On the other hand, HD-PPPV has a small electron affinity of 3.13 eV compared to 3.34 and 3.31 eV in HD-PPTV and PPTPV, respectively. Thus, HD-PPPV shows a much larger electrochemical bandgap of 2.35 eV than 1.80−1.90 eV of HD-PPTV and PPTPV. The EA and IP values of PPTPV are much similar and close to HD-PPTV since they share the same Th−DPP−Th core with strong intramolecular charge transfer. However, we noted that the current intensity for reduction curves was much lower than that of oxidation curves. The results suggested that the three DPP-based poly(arylene vinylene)s may be capable of charge transport of both holes and electrons in the solid state. However, they may have a better capability of transporting holes instead of electrons.

Field-Effect Transistors and Inverters. The charge transport properties of the three DPP-based poly(arylene vinylene)s were investigated by fabrication of organic field-effect transistors (OFETs). OFETs with bottom-contacts and bottom-gate geometry and gold source−drain electrodes were fabricated by spin-coating each polymer solution in 1,2-dichlorobenzene onto octyltrichlorosilane (OTS-8)-treated silicon/silicon dioxide substrates. Figure 5 shows representative output and transfer

Table 2. Electrical Parameters of HD-PPTV, HD-PPPV, and PPTPV Transistors

polymer	T_a[a] (°C)	μ_h[b] ($cm^2\ V^{-1}\ s^{-1}$)	μ_e[b] ($cm^2\ V^{-1}\ s^{-1}$)	$V_{t,h}$[b] (V)	$V_{t,e}$[b] (V)	I_{on}/I_{off}
HD-PPTV	110	0.11	0.015	−5.9	24.5	10^2-10^3
	150	0.17	0.017	−5.5	22.7	10^2-10^3
	200	0.14	0.019	−1.6	28.8	10^2-10^3
	250	0.091	0.012	−9.0	32.1	10^2-10^3
HD-PPPV	150	4.9×10^{-7}		−9.8		10^1
PPTPV	110	3.9×10^{-4}	2.9×10^{-6}	3.9	17.9	10^2-10^3
	150	2.2×10^{-3}	2.3×10^{-5}	−2.6	16.4	10^2-10^3
	200	1.5×10^{-3}	1.9×10^{-5}	−9.3	24.2	10^2-10^3

[a] The polymer film was annealed at T_a for 10 min. [b] Average of 5−6 devices.

characteristics of OFETs based on the DPP polymer semiconductors. HD-PPTV showed both hole and electron charge transport with typical ambipolar features (Figure 5A).[3b,20] Similar to HD-PPTV, the random copolymer PPTPV also showed ambipolar charge transport, whereas HD-PPPV showed only hole transport (Figure 5B). The charge-carrier mobilities were calculated from transfer curves using the standard saturation region equation of field-effect transistors: $I_{ds} = (\mu WC_o/2L)(V_g - V_t)^2$.[2,21] Ambipolar charge transport with hole mobility as high as 0.20 $cm^2\ V^{-1}\ s^{-1}$ and electron mobility as high as 0.03 $cm^2\ V^{-1}\ s^{-1}$ was observed in HD-PPTV. These mobilities are comparable to the highest reported so far for ambipolar OFETs based on a single conjugated polymer semiconductor.[5,8a,8g,8h] The hole mobility in the HD-PPTV OFETs is about 1 order of magnitude higher than the electron mobility. This may be a result of the larger injection barrier for electrons from the gold source/drain electrodes.

Figure 6 shows the hole and electron mobilities obtained from HD-PPTV OFETs that were thermally annealed at temperature ranging from 110 to 250 °C. The extracted electrical parameters are collected in Table 2. The average hole mobility was in the narrow range of 0.091−0.17 $cm^2\ V^{-1}\ s^{-1}$ and the average electron mobility was 0.012−0.019 $cm^2\ V^{-1}\ s^{-1}$ with current on/off ratios of 10^2-10^3. The maximum hole and electron mobilities were 0.20 and 0.03 $cm^2\ V^{-1}\ s^{-1}$, respectively. The threshold voltage of hole and electron transport are −9.0 to −1.6 V for p-channel operation and 22.7−32.1 V for n-channel mode. These asymmetric threshold voltages are commonly seen in ambipolar OFETs based on DPP-containing polymers.[5,8a,8f,8g] The measured hole/electron mobility is insensitive to the annealing temperature (T_a). We believe that thermal annealing did not have a substantial influence on charge transport because of the lack of a clear glass or melting transition in the DSC scans of HD-PPTV up to 350 °C. We note that a brief exposure of the devices to air before test (less than 2 min) caused a decrease of both hole and electron mobilities by factors of 1.5−3 and 2−14, respectively, resulting in average mobilities of 0.04−0.12 $cm^2\ V^{-1}\ s^{-1}$ for holes and 0.001−0.006 $cm^2\ V^{-1}\ s^{-1}$ for electrons (Figure 6). The large decrease of electron mobility in air is likely due to the relatively high-lying LUMO energy level (−3.34 eV), which would mean that electrons are trapped in oxygen preferentially than move in the polymer.[22] The presence of the dopants may also affect the hole transport.

In the case of HD-PPPV, the average hole mobility of 4.9×10^{-7} $cm^2\ V^{-1}\ s^{-1}$ was obtained and electron transport was not observed in the OFETs. A major reason for the lack of electron transport in HD-PPPV is its high-lying LUMO level (−3.13 eV), resulting in a large injection barrier for electrons from the gold electrodes. In addition, the largely amorphous nature of HD-PPPV thin film also accounts for the poor charge transport in the material. PPTPV had a compromised OFET performance with average hole and electron mobilities of 3.9×10^{-4} to 2.2×10^{-3} and 2.9×10^{-6} to 2.3×10^{-5} $cm^2\ V^{-1}\ s^{-1}$, respectively, after annealing at 110−200 °C, summarized in Table 2. The highest average mobilities in PPTPV OFETs were observed after annealing at 150 °C (Table 2).

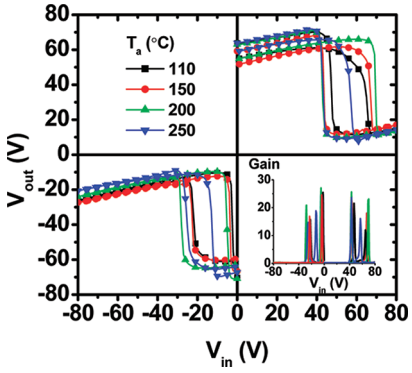

Figure 7. Voltage transfer characteristics of complementary inverters based on HD-PPTV OFETs after annealing at various temperatures (T_a). The inset shows the plot of gain ($-dV_{out}/dV_{in}$) that corresponds to the voltage transfer curves.

In light of the ambipolar field-effect charge transport in HD-PPTV, complementary inverters were successfully fabricated and demonstrated by integrating two transistors on a substrate with a shared gate. The same device configuration and applied biases were employed following our previous report.[2b] Figure 7 shows the voltage transfer characteristics (V_{out} vs V_{in}) of the inverters with a supplied voltage (V_{dd}) of ±80 V after annealing at various temperatures. Signal switching in an ideal inverter occurs at a half of V_{dd}. However, the inverter based on HD-PPTV showed switching at voltages more positive than $V_{dd}/2$ because of the positive threshold voltages of the individual transistor. Nevertheless, the inverters showed sharp switching characteristics with a voltage gain ($-dV_{out}/dV_{in}$) of 15−27. The hysteresis between forward and reverse sweeps may be a result of the asymmetry of charge carrier mobilities and the asymmetry of threshold voltages in p- and n-channel operation.[21]

CONCLUSIONS

New poly(arylene vinylene)s based on diketopyrrolopyrrole central unit were synthesized and characterized. Introduction of

dx.doi.org/10.1021/cm202247a |Chem. Mater. 2011, 23, 4618–4624

vinylene linkages in DPP-based donor−acceptor copolymers resulted in small bandgaps, enhanced conjugated length, and good charge transport. HD-PPTV with a highly crystalline morphology showed excellent hole and electron charge transport. Utilization of the new polymer semiconductors in thin film transistors led to the achievement of ambipolar charge transport with very high hole and electron mobilities (0.20 and 0.03 $cm^2 V^{-1} s^{-1}$) in HD-PPTV. Output voltage gains as high as 15−27 with sharp signal switching characteristics were seen in complementary inverters assembled from the ambipolar HD-PPTV transistors. These results suggest that poly(arylene vinylene)s containing DPP core are promising semiconductors with tunable electronic structure and charge transport properties for applications in organic electronics.

■ ASSOCIATED CONTENT

Supporting Information. ^{1}H NMR spectra of two monomers (**m1** and **m2**) and DSC scans of DPP copolymers (PDF). This information is available free of charge via the Internet at http://pubs.acs.org/.

■ AUTHOR INFORMATION

Corresponding Author
*E-mail: jenekhe@u.washington.edu.

■ ACKNOWLEDGMENT

Our report is based on research supported by the NSF (DMR-0805259) and Solvay S. A., and in part by the Office of Naval Research.

■ REFERENCES

(1) (a) van Mullekom, H. A. M.; Vekemans, J. A. J. M.; Havinga, E. E.; Meijer, E. W. *Mater. Sci. Eng. R.* **2001**, *32*, 1. (b) Jenekhe, S. A.; Lu, L.; Alam, M. M. *Macromolecules* **2001**, *34*, 7315. (c) Kroon, R.; Lenes, M.; Hummelen, J. C.; Blom, P. W.; de Boer, B. *Polym. Rev.* **2008**, *48*, 531.

(2) (a) Guo, X.; Kim, F. S.; Jenekhe, S. A.; Watson, M. D. *J. Am. Chem. Soc.* **2009**, *131*, 7206. (b) Kim, F. S.; Guo, X.; Watson, M. D.; Jenekhe, S. A. *Adv. Mater.* **2010**, *22*, 478. (c) Xin, H.; Guo, X.; Kim, F. S.; Ren, G.; Watson, M. W.; Jenekhe, S. A. *J. Mater. Chem.* **2009**, *19*, 5303. (d) Guo, X.; Watson, M. D. *Org. Lett.* **2008**, *10*, 5333.

(3) (a) Wu, P.-T.; Bull, T.; Kim, F. S.; Luscombe, C. K.; Jenekhe, S. A. *Macromolecules* **2009**, *42*, 671. (b) Blouin, N.; Michaud, A.; Gendron, D.; Wakim, S.; Blair, E.; Neagu-Plesu, R.; Belletête, M.; Durocher, G.; Tao, Y.; Leclerc, M. *J. Am. Chem. Soc.* **2008**, *130*, 732. (c) Yu, C.-Y.; Chen, C.-P.; Chan, S.-H.; Hwang, G.-W.; Ting, C. *Chem. Mater.* **2009**, *21*, 3262.

(4) (a) Letizia, J. A.; Salata, M.; Tribout, C.; Facchetti, A.; Ratner, M. A.; Marks, T. J. *J. Am. Chem. Soc.* **2008**, *130*, 9679. (b) Zhan, X.; Tan, Z.; Domercq, B.; An, Z.; Zhang, X.; Barlow, S.; Li, Y.; Zhu, D.; Kippelen, B.; Marder, S. R. *J. Am. Chem. Soc.* **2007**, *129*, 7246. (c) Zhang, Q. T.; Tour, J. M. *J. Am. Chem. Soc.* **1997**, *119*, 5065. (d) Zou, Y.; Najari, A.; Berrouard, P.; Beaupre, S.; Reda Aich, B.; Tao, Y.; Leclerc, M. *J. Am. Chem. Soc.* **2010**, *132*, 5330.

(5) Bürgi, L.; Turbiez, M.; Pfeiffer, R.; Bienewald, F.; Kirner, H.-J.; Winnewisser, C. *Adv. Mater.* **2008**, *20*, 2217.

(6) (a) Zhu, Y.; Rabindranath, A. R.; Beyerlein, T.; Tieke, B. *Macromolecules* **2007**, *40*, 6981. (b) Cao, D.; Liu, Q.; Zeng, W.; Han, S.; Peng, J.; Liu, S. *J. Polym. Sci:. Part A, Polym. Chem.* **2006**, *44*, 2395.

(7) (a) Wienk, M. M.; Turbiez, M.; Gilot, J.; Janssen, R. A. J. *Adv. Mater.* **2008**, *20*, 2556. (b) Zhou, E.; Yamakawa, S.; Tajima, K.; Yang, Z.; Hashimoto, K. *Chem. Mater.* **2009**, *21*, 4055. (c) Huo, L.; Hou, J.; Chen, H.-Y.; Zhang, S.; Jiang, Y.; Chen, T. L.; Yang, Y. *Macromolecules* **2009**, *42*, 6564. (d) Chen, G.-Y.; Chiang, C.-M.; Kekuda, D.; Lan, S.-C.; Chu, C.-W.; Wei, K.-H. *J. Polym. Sci:. Part A, Polym. Chem.* **2010**, *48*, 1669. (e) Kanimozhi, C.; Balraju, P.; Sharma, G. D.; Patil, S. *J. Phys. Chem. B* **2010**, *114*, 3095.

(8) (a) Bijleveld, J. C.; Zoombelt, A. P.; Mathijssen, S. G. J.; Wienk, M. M.; Turbiez, M.; de Leeuw, D. M.; Janssen, R. A. J. *J. Am. Chem. Soc.* **2009**, *131*, 16616. (b) Zou, Y.; Gendron, D.; Badrou-Aïch, R.; Najari, A.; Tao, Y.; Leclerc, M. *Macromolecules* **2009**, *42*, 2891. (c) Yu, C.-Y.; Chen, C.-P.; Chan, S.-H.; Hwang, G.-W.; Ting, C. *Chem. Mater.* **2009**, *21*, 3262. (d) Zhou, E.; Wei, Q.; Yamakawa, S.; Yang, Z.; Tajima, K.; Yang, C.; Hashimoto, K. *Macromoleclules* **2010**, *43*, 821. (e) Allard, N.; Badrou-Aïch, R.; Gendron, D.; Boudreault, P.-L. T.; Tessier, C.; Alem, S.; Tse, S.-C.; Tao, Y.; Leclerc, M. *Macromolecules* **2010**, *43*, 2328. (f) Zoombelt, A. P.; Mathijssen, S. G. J.; Turbiez, M. G.; Wienk, M. M.; Janssen, R. A. J. *J. Mater. Chem.* **2010**, *20*, 2240. (g) Tsai, J.-H.; Lee, W.-Y.; Chen, W.-C.; Yu, C.-Y.; Hwang, G.-H.; Ting, C. *Chem. Mater.* **2010**, *22*, 3290. (h) Sonar, P.; Singh, S. P.; Li, Y.; Soh, M. S.; Dodabalapur, A. *Adv. Mater.* **2010**, *22*, 5409. (i) Li, Y.; Sonar, P.; Singh, S. P.; Soh, M. S.; van Meurs, M.; Tan, J. *J. Am. Chem. Soc.* **2011**, *133*, 2198. (j) Ha, T.-J.; Sonar, P.; Dodabalapur, A. *Appl. Phys. Lett.* **2011**, *98*, 253305.

(9) (a) Tamayo, A. B.; Tantiwiwat, M.; Walker, B.; Nguyen, T.-Q. *J. Phys. Chem. C* **2008**, *112*, 15543. (b) Tamayo, A. B.; Dang, X.-D.; Walker, B.; Seo, J.; Kent, T.; Nguyen, T.-Q. *Appl. Phys. Lett.* **2009**, *94*, 103301. (c) Walker, B.; Tamayo, A. B.; Dang, X.-D.; Zalar, P.; Seo, J. H.; Garcia, A.; Tantiwiwat, M.; Nguyen, T.-Q. *Adv. Funct. Mater.* **2009**, *19*, 3063.

(10) (a) Smith, H. M. *High Performance Pigments*; Wiley-VCH: Weinheim, 2002. (b) Fukuda, M.; Kodama, K.; Yamamoto, H.; Mito, K. *Dyes Pigm.* **2004**, *63*, 115.

(11) (a) Tylleman, B.; Gbabode, G.; Amato, C.; Buess-Herman, C.; Lemaur, V.; Cornil, J.; Aspe, R. G.; Geerts, Y. H.; Sergeyev, S. *Chem. Mater.* **2009**, *21*, 2789. (b) Ahmed, E.; Kim, F. S.; Xin, H.; Jenekhe, S. A. *Macromolecules* **2009**, *42*, 8615. (c) Zhu, Y.; Champion, R. D.; Jenekhe, S. A. *Macromolecules* **2006**, *39*, 8712.

(12) (a) Rabindranath, A. R.; Zhu, Y.; Heim, I.; Tieke, B. *Macromolecules* **2006**, *39*, 8250. (b) Liu, K.; Li, Y.; Yang, M. *J. Appl. Polym. Sci.* **2009**, *111*, 1976.

(13) Jenekhe, S. A.; Alam, M. M.; Zhu, Y.; Jiang, S.; Shevade, A. V. *Adv. Mater.* **2007**, *19*, 536–542.

(14) (a) Jenekhe, S. A.; Osaheni, J. A. *Science* **1994**, *265*, 765. (b) Osaheni, J. A.; Jenekhe, S. A. *Macromolecules* **1994**, *27*, 739.

(15) Wu, P.-T.; Ren, G.; Jenekhe, S. A. *Macromolecules* **2010**, *43*, 3306.

(16) Sonar, P.; Ng, G.-M.; Lin, T. T.; Dodabalapur, A.; Chen, Z.-K. *J. Mater. Chem.* **2010**, *20*, 3626.

(17) (a) Vala, M.; Vyňuchal, J.; Toman, P.; Weiter, M.; Luňák, S., Jr. *Dyes Pigm.* **2010**, *84*, 176. (b) Morton, C. J. H.; Gilmour, R.; Smith, D. M.; Lightfoot, P.; Slawin, A. M.; Maclean, E. J. *Tetrahedron* **2002**, *58*, 5547.

(18) The ionization potential was calculated as IP = eE_{ox}^{onset} + 4.4 eV and the electron affinity was calculated as LUMO = eE_{red}^{onset} + 4.4 eV. See ref 19.

(19) (a) Yang, C. J.; Jenekhe, S. A. *Macromolecules* **1995**, *28*, 1180. (b) Kulkarni, A. P.; Tonzola, C. J.; Babel, A.; Jenekhe, S. A. *Chem. Mater.* **2004**, *16*, 4556.

(20) (a) Babel, A.; Wind, J. D.; Jenekhe, S. A. *Adv. Funct. Mater.* **2004**, *14*, 891. (b) Babel, A.; Zhu, Y.; Cheng, K.-F.; Chen, W.-C.; Jenekhe, S. A. *Adv. Funct. Mater.* **2007**, *17*, 2542.

(21) Kang, S.-M.; Leblebici, Y. *CMOS Digital Integrated Circuits: Analysis and Design*; McGraw-Hill: New York, 1996.

(22) (a) Briseno, A. L.; Mannsfeld, S. C. B.; Shamberger, P. J.; Ohuchi, F. S.; Bao, Z.; Jenekhe, S. A.; Xia, Y. *Chem. Mater.* **2008**, *20*, 4712. (b) Newman, C. R.; Frisbie, C. D.; da Silva Filho, D. A.; Brédas, J.-L.; Ewbank, P. C.; Mann, K. R. *Chem. Mater.* **2004**, *16*, 4436.